JOINT INSTITUTE FOR NUCLEAR RESEARCH

FINAL REPORT ON THE INTEREST PROGRAMME

Radiation effects study on MWCNT exposed to electron beam and gamma rays using the Raman Spectroscopy

Supervisor:
Dr. Antonio Leyva Fabelo

Student:
Lic. Deniel Rodriguez Almora
High Institute of Technologies and Applied Sciences, La Havana ,Cuba.

Participation period:
November 05 - December 14
Wave 11

Dubna, 2024

Abstract

Raman spectroscopy is a powerful analytical technique used to investigate the vibrational modes of molecules, providing insights into molecular structures and interactions. This study explores the application of Raman spectroscopy to multi-walled carbon nanotubes (MWCNTs) before and after irradiation with gamma rays and electrons. The analysis reveals significant structural changes in the MWCNTs post-irradiation, characterized by shifts in peak intensities, particularly in the D and G bands, which indicate variations in defect densities and structural integrity. Utilizing mathematical deconvolution techniques, the study identifies key spectral features and their implications for the material's quality and potential applications in nanotechnology and materials science.

Introduction

Raman spectroscopy is a powerful and versatile analytical technique that has revolutionized the field of chemistry and other scientific disciplines since its discovery. Based on the phenomenon of inelastic photon scattering, this technique allows for the analysis of molecular vibrations, providing detailed structural information about various substances. While its initial applications relied on rudimentary methods and limited light sources, technological advancements have established Raman spectroscopy as a standard tool in laboratories worldwide.

The introduction of stable and cost-effective lasers in the 1980s, along with modern detectors such as charge-coupled devices (CCDs), has dramatically improved the sensitivity and resolution of this technique. These innovations have enabled researchers to obtain high-quality spectra in much shorter times, facilitating the study of complex molecules in various matrices.

The ability of Raman spectroscopy to identify molecular structures and analyze chemical interactions makes it an invaluable tool across multiple fields. Despite its numerous advantages, Raman spectroscopy faces certain challenges, such as the need to separate the Raman scattering signal from the intense Rayleigh light and other noise. However, the use of advanced filters and Fourier Transform techniques has enabled researchers to overcome these obstacles, making Raman spectroscopy more accessible and effective.

This paper will explore the fundamental principles of Raman spectroscopy, its applications across different fields, and discuss the technological advancements that have facilitated its development.

Material and Methods

Raman spectroscopy

Raman spectroscopy is a spectroscopic technique primarily used to determine the vibrational modes of molecules, although it can also observe rotational modes and other low-frequency vibrations. This technique relies on the inelastic scattering of photons, known as Raman scattering. The process begins with a laser that emits monochromatic light, typically in the visible, near-infrared, or near-ultraviolet range, which interacts with the molecular vibrations in the sample. This interaction causes a shift in the energy of the photons, allowing for the extraction of information about the vibrational modes present.

In practice, a laser illuminates the sample, and the resulting electromagnetic radiation is collected using a lens and sent through a monochromator. The scattered light is filtered to remove the elastic radiation associated with the laser light (known as Rayleigh scattering), using filters that may be bandpass, notch, or edge filters. Historically, Raman spectrometers used holographic gratings and multiple dispersion stages to achieve a high degree of laser rejection, complicating the collection of spectra due to the weak nature of Raman scattering.

Variations of Raman spectroscopy include surface-enhanced Raman (SERS), resonance Raman, and polarized Raman, among others. The magnitude of the Raman effect correlates with the polarizability of the electrons in a molecule, and the intensity of Raman scattering is proportional to the change in polarizability. This means that the Raman spectrum, which shows scattering intensity as a function of frequency shifts, depends on the rovibronic (rotational-vibrational-electronic) states of the molecule.

The Raman effect should not be confused with emission (fluorescence or phosphorescence), where a molecule in an excited state emits a photon as it returns to a ground electronic state. It also differs from infrared absorption, where the energy of the absorbed photon matches the energy difference between the initial and final rovibronic states. This distinction allows transitions that may not be active in IR to be analyzed using Raman spectroscopy.

The availability of reliable, stable, and inexpensive lasers with narrow bandwidths has also had a significant impact. Generally, shorter wavelength lasers produce stronger Raman scattering due to an increase in the Raman scattering cross-section, although this can lead to issues with sample degradation or fluorescence.

Continuous wave lasers are most commonly used for normal Raman spectroscopy, but pulsed lasers may also be employed, especially for advanced forms of Raman spectroscopy such as transient, time-resolved, and resonance Raman. The Raman scattered light is typically collected and either dispersed by a spectrograph or

detected using an interferometer with Fourier Transform (FT) methods. Many commercially available FT-IR spectrometers can be modified to function as FT-Raman spectrometers.

To obtain high-quality Raman spectra, it is usually necessary to separate the Raman scattered light from the Rayleigh signal and the reflected laser signal using laser rejection filters, such as notch or long-pass optical filters. Before the advent of holographic filters, a triple-grating monochromator in subtractive mode was commonly used to isolate the desired signal. However, volume hologram filters are becoming more prevalent, allowing for the observation of shifts as small as 5 cm^{-1}.[1] [2]

Applications of Raman Spectroscopy

Raman spectroscopy has numerous applications across various fields, including:

- **Chemistry:** Identification of substances and analysis of molecular structures.
- **Biology:** Study of biomolecules and analysis of biological tissues.
- **Materials Science:** Characterization of organic and inorganic materials.
- **Pharmaceuticals:** Quality control and analysis of compounds in medications.
- **Nanotechnology:** Analysis of materials at the nanoscale and studies of graphene.
- **Food Industry:** Assessment of quality and authenticity of food products.

MWCNT

Multi-walled carbon nanotubes (MWCNTs) consist of several concentric layers of graphene rolled into cylindrical shapes, with diameters reaching tens of nanometers. Their structure can be described using two primary models: the Russian Doll model, where graphite sheets are arranged in concentric cylinders with smaller single-walled nanotubes (SWNTs) nested inside larger ones, and the Parchment model, resembling a single sheet of graphite rolled into a scroll-like form. The interlayer distance in MWCNTs is approximately 3.4 Å, similar to the spacing between adjacent planes in crystalline graphite, typically characterized by a distance of about 0.34 nm between nearest graphene layers.

The Russian Doll structure is more commonly observed, and each layer can be classified as either metallic or semiconducting. Due to statistical variations in their diameters, at least one shell of the MWCNT generally behaves as a zero-gap metal. Additionally, the inner shells of MWCNTs possess the ability to move telescopically, functioning as low-friction bearings and nanosprings. This telescopic motion, facilitated by the Lennard-Jones interaction between layers, generates a retraction force of approximately 1.5 nN, making MWCNTs particularly appealing for

applications in nanoelectromechanical systems (NEMS), where precision and minimal wear are essential.

While MWCNTs are significant for their structural integrity and mechanical properties, they may also exhibit defects in their structure. These defects can sometimes lead to undesirable effects; however, in certain applications—such as hydrogen storage, enhancing chemical reactions, welding, and crosslinking—defective structures may be advantageous. MWCNTs can be characterized by Raman spectroscopy, which reveals two key peaks: the D band, indicative of disorder, and the G band, associated with the in-plane vibration of sp^2 (The sp^2 hybridization implies that a carbon atom is bonded to three other atoms (or groups) via covalent bonds, forming a trigonal planar structure. This is typical in structures such as graphene and graphite, where carbon atoms are organized in rings and chains.) carbon atoms. The D band intensity increases with the number of defects in the structure, suggesting that a higher concentration of defects leads to greater disorder. This relationship is crucial for assessing the quality of the nanotubes. The G band does not disperse in well-ordered graphite but can shift in disordered carbon structures, with dispersion correlating to the degree of disorder present.[3]

In this project, the analyzed MWCNT powder samples were commercial and 90% pure, indicating that while they possess structural integrity, they may also contain defects that could be beneficial for specific applications.[4]

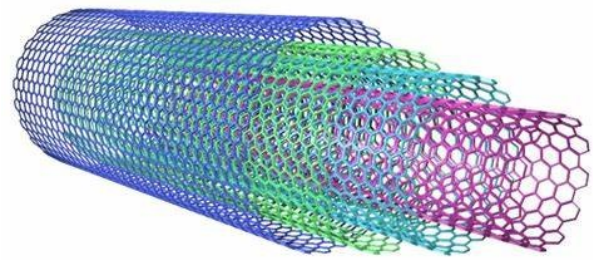

Figure 1: Structure of multi-walled carbon nanotube.

Irradiation facilities

Irradiation with photons of 1.25 MeV (^{60}Co) was performed in a therapeutic gamma chamber POKYEM available at the Medical Complex of the DLNP at the Joint Institute for Nuclear Research (JINR).

Figure 2: Radiotherapy chamber similar to the one used in the experiment.

The dose power of the chamber is 148.47 Gy/h. The total exposure dose of the irradiated samples was 23.4 kGy.

The photo in Figure 2 shows the equipment used, and the exposure to radiation was done by rotating the head so that the window was directed upwards and the samples were placed directly on top of it. The irradiation time was selected so that the samples received the relevant exposure dose.

Electron irradiation was performed on the JINR LINAC-800 linear accelerator Its general scheme is presented in Figure 3. The picture in Figure 4 presents a panoramic view of the accelerator.

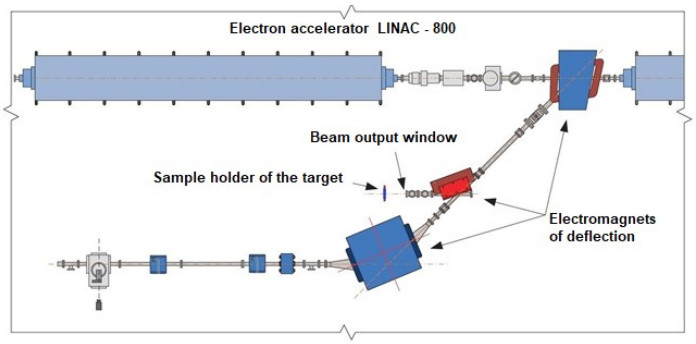

Figure 3: Overview of the LINAC-800 accelerator and the 20 MeV irradiation station.

Figure 4: Panoramic view of the LINAC-800 linear accelerator.

The samples were placed directly in front of the electron output Ti window. The parameters of the beam are energy 20 MeV, current 10 mA, frequency 10 Hz, and pulse duration 1.5 μs. The fluence in the sample was 4.38×10^{18} e^{-} cm^{-2}.

Raman spectrometer

The Raman measurements were done at room temperature in backscattering geometry regime, using a spectrometer model Solar TII (see Figure 5), applying the following conditions: diffraction grating of 1200 lines/mm, objective 40x (model Olympus-UPlanFL N), and acquisition time 70 s.[5]

Figure 5: Solar TII Raman spectrometer setup.

Mathematical processing

The post-processing of the spectra was carried out using the ORIGIN software package, which is widely used for data analysis and visualization in scientific research. Initially, the data obtained from the measurements were normalized to ensure consistency, allowing for accurate comparisons between different spectra. This normalization process adjusts the intensity values so that variations due to experimental conditions do not obscure the inherent differences in the sample properties. Once normalized, the spectra were plotted on the same graph, facilitating a clear visual comparison of the changes that occur after irradiation. This approach enables researchers to identify and analyze trends or discrepancies in the data more effectively. Each spectrum underwent a process known as deconvolution, which is crucial for extracting detailed information from overlapping peaks. Deconvolution involves separating these peaks to identify their individual contributions and intensities, which can be obscured in dense spectral regions. This technique is essential for understanding complex molecular interactions and obtaining precise measurements of peak characteristics. For the Raman spectrum specifically, the deconvolution was performed using the Voigt fitting function. This function combines

the effects of both Gaussian and Lorentzian profiles, providing a more accurate representation of the peaks. By applying this fitting method, we could effectively resolve overlapping peaks and quantify their intensities, leading to a clearer interpretation of the spectral data and enhancing our understanding of the underlying molecular structures. The use of Gaussian or Lorentzian functions alone did not yield satisfactory results. Consequently, the deconvolution process was performed using the Voigt mathematical function, which combines a Cauchy-Lorentz distribution with a Gaussian distribution. The defining integral is expressed as:

$$V(x;\sigma,\gamma)=\int_{-\infty}^{\infty} G(x';\sigma)L(x-x';\gamma)dx',$$

where $G(x';\sigma)$and $L(x-x';\gamma)$ represent the Gaussian and Lorentz distributions, respectively. This integral can be evaluated as:

$$V(x;\sigma,\gamma)=\frac{\left(Re\left[w(z)\right]\right)}{\sigma\sqrt{(2\pi)}},$$

with Re[w(z)] being the real part of the Faddeeva function for:

$$z=x+\frac{(i\gamma)}{\sigma\sqrt{2}}$$

By employing the Voigt function, we account for the two primary mechanisms that cause broadening of transition lines: "homogeneous broadening," which results in Gaussian shapes, and "inhomogeneous broadening," which leads to Lorentzian shapes.

Interaction of gamma quanta and light particles with matter

Gamma rays, which are a type of shortwave electromagnetic radiation (10 keV – 10 MeV), are emitted by unstable nuclei when they transition from a high-energy state to a lower state (gamma decay). The interaction of gamma rays and light particles (photons) with matter occurs through several physical processes. The main mechanisms include the photoelectric effect, which occurs when a high-energy photon interacts with an electron in an atom, freeing it from the atom; this process is more likely in materials with high atomic numbers and for lower-energy photons. Another mechanism is Compton scattering, where a photon interacts with a free or loosely bound electron, scattering with less energy, which is relevant for intermediate-energy photons. Additionally, pair production can occur when photon energy exceeds 1.022 MeV, allowing the photon to convert into a pair of particles: an electron and a positron, typically in strong electromagnetic fields. Rayleigh scattering

is an elastic scattering process where photons interact with atoms without losing energy, maintaining their wavelength, and is more relevant for low-energy photons. Raman scattering refers to the inelastic scattering of photons, where interaction with molecular vibrations in matter causes a change in the energy of the photons, allowing for the acquisition of information about molecular structures and playing a fundamental role in spectroscopy. Lastly, absorption occurs when matter completely absorbs the energy of photons, resulting in an increase in the energy of the material and generating effects such as heating. Gamma decay typically accompanies other forms of decay, such as alpha or beta decay.[6]

Results and discussion

After overlaying two spectra (the spectrum of the sample before and after irradiation with two different sources: gamma rays and electrons) in Figures 6 and 7, a brief examination reveals that the spectra do not significantly differ in the position of the main peaks. However, at this initial glance, a noticeable difference in peak intensities can be observed. This variation suggests that some structural changes occurred following the material's irradiation. The deconvolution process applied to these spectra can provide deeper insights into the involved processes.

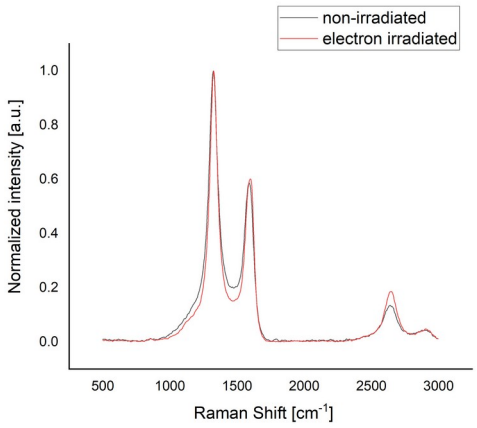

Figure 6: Raman spectrum of MWCNT sample before and after electrons exposure. Each peak is identified with the most probable mode it represents

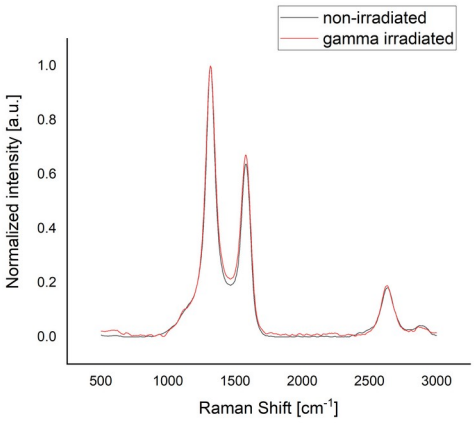

Figure 7: Raman spectrum of MWCNT sample before and after gamma rays exposure. Each peak is identified with the most probable mode it represents

The deconvoluted spectra are displayed in Figures 8, 9, 10, and 11, while the various parameters extracted from them, characterizing each fitted peak or mode, are

presented in Tables 1 and 2. The D mode appears in sp^2 carbon samples that contain pores, impurities, or other defects in the graphitic structure (defect-dependent). Generally, a higher number of defects correlates with an increased intensity of the D band. Therefore, we can conclude that both after gamma irradiation and electron irradiation, the number of defects in the MWCNT structure increased, as indicated by the heightened intensity of the D mode.

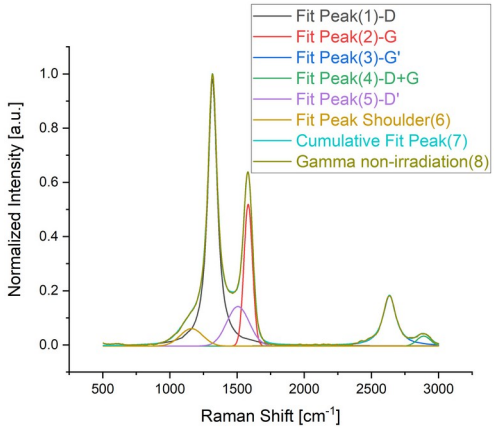

Figure 8: The deconvoluted Raman spectrum of MWCNT with its component peaks, before Gamma irradiation

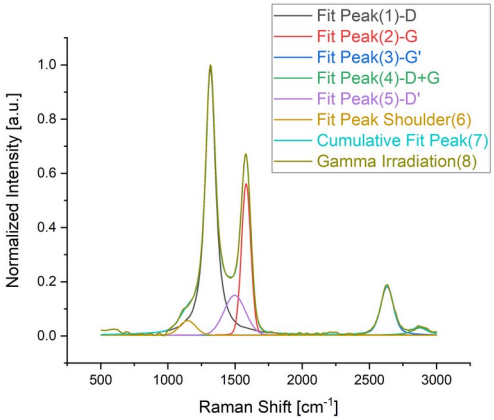

Figure 9: The deconvoluted Raman spectrum of MWCNT with its component peaks, after irradiation with ^{60}Co photons

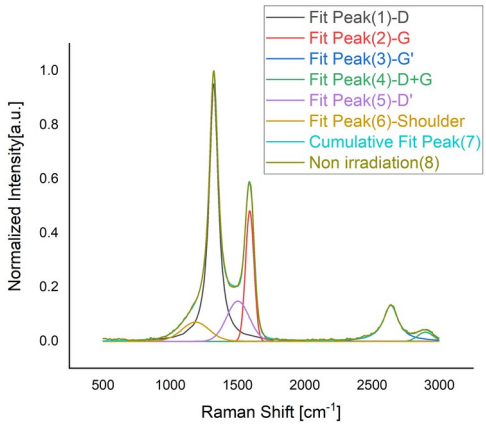

Figure 10: The deconvoluted Raman spectrum of MWCNT with its component peaks, before electron irradiation

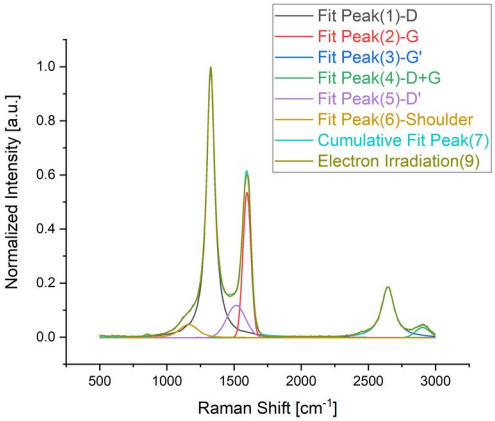

Figure 11: The deconvoluted Raman spectrum of MWCNT with its component peaks after irradiation with 20 MeV electrons

The G mode arises from the tangential vibrational motion of sp^2 carbon atoms. This peak does not disperse in pure graphite or glassy carbon but does disperse in more disordered carbon, where the dispersion is proportional to the disorder degree. The G peak dispersion divides materials into two types: in materials with only sp^2 rings, the G peak dispersion saturates at a maximum of 1600 cm^{-1}. In contrast, materials containing sp^2 chains exhibit a G peak that can rise beyond 1600 cm^{-1}, potentially reaching 1690 cm^{-1}. Thus, our material, both before and after irradiation, contains only sp^2 rings.

Table 1: Raman shifts of the analyzed spectra main modes

Raman shift [cm^{-1}]	Electron irradiation		Gamma irradiation	
	No irradiated	irradiated	No irradiated	irradiated
D mode	1323.20745	1326.08925	1317.5426	1317.0423
G mode	1591.62551	1594.66729	1583.10662	1582.81824
D’ mode	1502.76259	1499.47078	1507.01685	1497.46213
G’ mode	2639.54065	2645.27904	2634.71931	2631.79646
D+G mode	2896.01061	2907.10028	2889.40437	2876.43179

The ratio of the intensities of the D and G bands serves as a reliable indicator of the quality of bulk samples, characterizing the degree of graphitization of carbon materials and allowing us to determine the disorder level of the CNT samples. As illustrated in Figures 8, 9, 10, 11 and in Table 2, the intensity ratio of the D and G bands in all cases exceeds 1 (approximately 1.809 as average): the D band is more intense than the G band, indicating the presence of structural defects in the carbon nanotubes. Table 2 shows that after irradiation, this ratio decreased slightly, suggesting a reduction in structural defects within the multilayer nanotubes.

Table 2: Intensities of the analyzed spectra main modes.

Intensity [a.u.]	Electron irradiation		Gamma irradiation	
	No irradiated	irradiated	No irradiated	irradiated
D mode	0.98202	0.9733	0.98422	0.98368
G mode	0.50086	0.59561	0.52289	0.5581
D’ mode	0.13933	0.06916	0.14609	0.14678
G’ mode	0.13032	0.18584	0.18669	0.17844
D+G mode	0.03437	0.04115	0.03684	0.02716
ID/IG	1.96066	1.63412	1.88226	1.76255

Additionally, we observe an increase in the intensity of the G’ mode in both cases following irradiation. This mode is utilized to assess the quality of the nanotube material structure and can effectively characterize the material's crystallinity; thus, a decrease in its intensity after irradiation indicates a reduction in the number of defects. This phenomenon is more pronounced in the case of electron irradiation (exposure to 20 MeV electrons). The intensity of the G’ mode is closely linked to the number of tube layers, making it a frequent choice for layer determination. Our experiments show that both types of irradiation contribute not only to an enhancement in the quality of the multilayer material but also to its exfoliation, with a more significant effect observed in the case of electron irradiation.[7]

Finally, the deconvolution of the spectra not only provides reliable information on the intensity and shift of each mode that could be visually identified and analyzed but also reveals two peaks that had not been previously recognized. These include the D’ mode associated with amorphous sp^2-bonded carbon forms, and a "low-frequency shoulder" whose origin remains unclear. This shoulder likely arises from a double resonance process, as its Raman shift (~1150 cm^{-1}) corresponds to a point on phonon dispersion.[8][9]

Conclusions

Irradiation Effects on MWCNT Structure: The study demonstrates that both gamma and electron irradiation significantly influence the structural characteristics of multi-walled carbon nanotubes (MWCNTs). While the increase in D mode intensity indicates the introduction of defects such as pores and impurities, the overall decrease in the intensity ratio of the D and G bands suggests a reduction in structural defects post-irradiation.

1. **Peak Identification and Analysis**: Through detailed deconvolution of the Raman spectra, six key peaks (shoulder, D, D’, G, G’, and G+D) were identified, providing a comprehensive understanding of the vibrational modes present. The analysis of these peaks reveals valuable information about the material's disorder and graphitization levels.
2. **Material Quality and Graphitization**: The G’ mode, linked to graphitization and the number of nanotube layers, exhibited specific behavior post-irradiation. The results indicate that electron irradiation leads to more significant exfoliation and improvement in material quality compared to gamma irradiation, emphasizing the effectiveness of electron exposure for enhancing the structural properties of MWCNTs.
3. **Application in Advanced Materials**: The findings underscore the utility of Raman spectroscopy as a critical tool for assessing the structural integrity and quality of advanced materials like MWCNTs. The ability to discern subtle changes in vibrational modes and defect densities positions this technique as essential for optimizing carbon-based nanomaterials for various applications in nanotechnology and materials science.
4. **Future Research Directions**: The identification of new spectral features, including the D’ mode and low-frequency shoulder, suggests areas for further investigation. Understanding these components could provide deeper insights into the interactions and properties of irradiated carbon nanotubes, paving the way for innovative applications and enhancements in nanomaterial technologies.

References

1. M. S. Dresselhaus, G. Dresselhaus, R. Saito and A. Jorio. Raman spectroscopy of carbon nanotubes. Physics Reports 409 (2005) 47–99. DOI:10.1016/j.physrep.2004.10.006
2. E. F. Antunes, A. O. Lobo, E. J. Corat, et al. Comparative study of first- and second-order Raman spectra of MWCNT at visible and infrared laser excitation. Carbon 44 (2006) 2202–2211. DOI:10.1016/j.carbon.2006.03.003
3. Joe Hodkiewicz, Thermo Fisher Scientific, Madison, WI, USA. Characterizing Carbon Materials with Raman Spectroscopy. Thermo Fisher Scientific Inc. Paper. Application Note: 51901. DOI:10.1016/j.thermo.2023.01.001
4. Sreekanth P. S. R., Acharyya K., Talukdar I., Kanagaraj, S. Studies on Structural Defects on 60 Co Irradiated Multi Walled Carbon Nanotubes. Procedia Materials Science, 6, 1967–1975. 2014. DOI:10.1016/j.mspro.2014.07.231
5. Bokobza L., Zhang J. Raman spectroscopic characterization of multiwall carbon nanotubes and of composites. Express Polymer Letters, 6(7), 601–608. 2012. DOI:10.3144/expresspolymlett.2012.63
6. Hans Bichsel, Heinrich Schindler. Chapter 2 The Interaction of Radiation with Matter. Particle Physics Reference Library. 5-44. 2020. DOI:10.1007/978-3-030-35318-6_2
7. X. Zhiwei, Ch. Lei, L. Liangsen, et al. Structural changes in multi-walled carbon nanotubes caused by γ-ray irradiation. Carbon 49(1) (2011) 339-351. DOI:10.1016/j.carbon.2010.09.023
8. B. Safibonaba, A. Reyhani, A. N. Golikand, et al. Improving the surface properties of multi-walled carbon nanotubes after irradiation with gamma rays. Applied Surface Science 258(2) (2011) 766-773. DOI:10.1016/j.apsusc.2011.08.085
9. R. A. DiLeo, B. J. Landi, and R. P. Raffaelle. Purity assessment of multiwalled carbon nanotubes by Raman spectroscopy. Journal of Applied Physics, 101(6) (2007) 064307. DOI:10.1063/1.2712152

Acknowledgments:

I would like to express my gratitude to the INTEREST Program for giving me the opportunity to participate and for allowing me to learn new things with excellent supervisors. I am especially thankful to my supervisor, Antonio Leyva Fabelo, for always being available to clarify any doubts that arose. Thank you from the bottom of my heart; I truly feel grateful and fortunate to have had this wonderful opportunity. I hope that this work will benefit future participants.